



Geotechnical design of a secant piled underground pump station in liquefiable ground

Dr. S. Ghanooni & J.W.S. Milford

ABuild Consulting Engineers Limited, Wellington, New Zealand.

ABSTRACT

The geotechnical design of underground structures with a high importance level, in a dense urban area, in liquefiable ground, and adjacent to existing structures that are sensitive to settlement is challenging because multiple model inputs need to be considered, many of which act concurrently. The new structure should consider each of these factors in both short and long term conditions, and in various combinations. This paper presents the design process undertaken by GHD Limited for an underground pump station located in central Wellington adjacent to existing sensitive structures in liquefiable ground. The overall stability of the proposed construction sequence was assessed, and resulting actions on the structural elements of the shaft for both short-term and long-term conditions were evaluated in the 3D finite element modelling (FEM) software, Plaxis 3D. The FEM based technique included a settlement assessment for the sensitive adjacent structures and provided structural actions for the design of the structural elements, in addition to assessing performance in a design level earthquake and subsequent liquefaction. The secant pile shaft provides very little deformation and settlement outside of the pile group, is able to resist very high loads from the surrounding structures, produces lower vibration during construction, and good watertightness considering high in situ groundwater levels.

1 INTRODUCTION

This paper presents the Taranaki Street Pump Station, Inglewood Place, Wellington (the Site) as a case study for the design of a large underground secant piled pump station in liquefiable ground. The Site (refer Figure 1) is located on the corner of Inglewood Place and Taranaki Street in Wellington CBD, adjacent to the existing Soho Apartments and Hope Gibbons Buildings. The pump station is part of a broader package of work that includes upgrades to the Taranaki Street rising main, both of which connect to the CBD interceptor main to provide an alternative connection to the interceptor and reduce neighbouring wastewater catchment sizes.

The pump station is 10.25m in diameter, with 42 No. 17m long secant piles forming the main structure. The base plug is founded at 8.50m below ground level.



Figure 1: Location Plan

2 SITE CHARACTERISTICS AND BACKGROUND INFORMATION

2.1 Ground model

A two-stage geotechnical investigation was completed at the site comprising a total of six (6) machine boreholes and two (2) cone penetrometer tests (CPTs) adjacent to, and within the footprint, of the proposed shaft. Testing extended to 30.16m depth at the deepest point. Supplementary laboratory testing comprising Atterberg Limits, moisture content and consolidated drained triaxial testing was also completed on undisturbed samples obtained using push tubes.

Piezometers were installed in the boreholes to obtain long-term groundwater levels and determine hydraulic conductivity. Groundwater was measured at between 1.98-2.75mBGL.

The site is located near the boundary of three distinct lithologies (Begg & Mazengarb, 1996); fr (Reclamation Fill), fa (Alluvium), and fm (Marginal Marine Sediments). The intrusive testing data indicate that the site is underlain by predominantly comprised of fill overlying alluvial soils, which broadly match the published geological map and geomorphology. Fill was logged from around 1.5mBGL and has been interpreted as reclamation fill.

The alluvial soils encountered comprised varying fractions of silt, sand and gravel, with trace clay.

The results of the intrusive testing, considered in conjunction with the guidance in NZS1170.5 (NZS, 2004), indicate that the site subsoil class is D – Deep or soft soil.

2.2 Importance Level, Design Life and Peak Ground Acceleration

The structure has been designated by the asset owner as Importance Level 4, with a 100 year design life (NZS, 2002). Given this classification the structure was the subject of a Site-Specific Seismic Hazard

Assessment (SSSHA), completed by Tonkin and Taylor (Balachandra, 2021), with design return periods, PGAs and magnitudes reproduced below in Table 1. The SSSHA was peer reviewed by Engineering Geology Limited.

Table 1: Ground motion parameters

| Return period (years) | Peak ground acceleration (g) | Magnitude (M_w) |
|------------------------------|-------------------------------------|----------------------------------|
| 25 | 0.15 | 6.3 |
| 100 | 0.28 | 7.0* |
| 250 | 0.46 | 7.1 |
| 500 | 0.62 | 7.4 |
| 1,000 | 0.82 | 7.6 |
| 2,500 | 1.15 | 7.9 |
| 5,000 | 1.45 | 8.0 |

* The magnitude has been linearly interpolated based on annual probability of exceedance (taken as approximately equal to 1 / return period).

Cumulative cyclic seismic displacements were provided as part of the SSSHA and applied to the model extents in the seismic stage.

WWL have been moving to make wastewater (and stormwater) structures IL3 since at least the end of 2021 due to the increase in seismic loadings and subsequent costs.

2.3 Surrounding Structures

The proposed pump station is located adjacent to existing buildings of varying age and construction type, with the foundation system of each structure determining their response to the proposed shaft.

1925 Hope Gibbons Building

This building was constructed in 1925 and is a 9 storey (with a basement), concrete encased steel frame structure with reinforced concrete wall panels that underwent strengthening in 2013. The structure is founded on shallow pads comprising a localised grid of steel girders. Hold down anchors were installed to the base of retrofitted shear walls as part of the strengthening programme.

1916 Hope Gibbons Building

The 1916 Hope Gibbons Building has a 5 storey, riveted steel framed gravity structure, with shallow foundations and an unreinforced masonry exterior, which is particularly sensitive to both differential settlement and construction vibration. The building was extended with an additional bay to the south in 1917.

Hope Gibbons Carpark

The Hope Gibbons carpark building was constructed in 1987 with a reinforced concrete frame and central shear core. The building included piles founded at 7 m BGL which, based on the findings from the recent intrusive investigations, are at a depth that is expected to liquefy during a seismic event which may cause rapid settlement, causing a large uniformly distributed load to be suddenly applied to the ground surface. This effect has been assessed during the Plaxis modelling.

Soho Apartments

Paper 38 – Geotechnical design of a secant piled underground pump station in liquefiable ground.

The Soho Apartments is a concrete framed apartment block built in 2009. Council records indicate that the foundations are piled with belled ends under all primary column lines to depths of between 13.6-16.0mBGL. The foundations are tied with ground beams creating a grillage immediately below ground level. The single level podium areas have shallow, un-piled foundations.

2.4 Liquefaction assessment

A liquefaction assessment was completed using CLiq (Boulanger & Idriss, 2014) that indicates multiple, discrete layers of material will liquefy, many of which are continuous across the testing locations and through the pump station location. Manifestation of the liquefaction effects at the site may include differential movement of pipe connections, uplift below the base plug, loss of bearing capacity/skin friction of the piles, ejecta causing differential settlement, and negative skin friction on the piles. These effects were considered during the detailed design.

2.5 Foundation options

Table 2 presents the foundation options considered for the pump station. The foundation options were determined in conjunction with the structural and water engineers, and considered cost, performance and constructability.

Table 2: Foundation options considered for the pump station

| Foundation option | Advantages | Disadvantages |
|-------------------|--|--|
| Caisson | <ul style="list-style-type: none"> • More reliable controls on joints between caisson elements • Cheaper | <ul style="list-style-type: none"> • Requires bentonite filled annulus between caisson and ground to install, with a loss of pressure potentially causing displacement • Requires excavation around drive shoe in difficult ground conditions, and associated dewatering • Availability of local production facilities for caisson elements |
| Secant Piles | <ul style="list-style-type: none"> • Effective groundwater control during construction • Low vibration construction • Generally smaller footprint required for construction • Top down temporary works support while excavating • Local availability of piling rigs | <ul style="list-style-type: none"> • Requires strict QAQC to ensure proper alignment and spacing of piles • Relative cost |

Ultimately a secant pile option was selected for detailed design due to this method producing very little deformation and settlement outside of the pile group, its ability to carry high loads from surrounding structures, low vibration construction, and good watertightness considering high in situ groundwater levels.

Secant piles are formed by installing intersecting reinforced concrete piles. The secant piles are reinforced with steel rebar and are constructed by augering. Primary (soft, cement-bentonite mix) piles are installed first with secondary piles (hard) constructed in between the primary piles once the latter gains sufficient strength.

Paper 38 – Geotechnical design of a secant piled underground pump station in liquefiable ground.

3 DETAILED DESIGN

Detailed geotechnical design of the pump station was undertaken using Plaxis 3D Finite Element Modelling (FEM) software with the model inputs and design process summarised below.

3.1 Soil and material properties

Design soil and material properties were determined using Plaxis SoilTest to derive the soil parameters for fine grain soils and simulate the actual laboratory test results.

A Hardening-Soil Model (H-S Model) was adopted, which accounts for stress dependency of stiffness moduli, captures plastic deformation in the soils from the early stages of loading and simulates hardening behaviour.

Liquefied material properties were based on Stark & Mesri (Stark & Mesri, 1992) as recommended by MBIE Module 1 (MBIE, 2021), with residual shear strengths of 8-11 kPa obtained (Eq. 1).

$$\frac{s_u(LIQ)}{\sigma_{vo}} = 0.0055(N1)_{60-CS} \quad (1)$$

Ciria R143 (Clayton, 1995) was used to establish the Young's modulus (E_{50}) for non-liquefied coarse-grained soils based on their SPT-N values.

Design soil parameters are presented in Table 3.

Table 3: Design soil parameters

| Parameters | Depth (m) | | | | | | | | | | |
|--|--------------------------------|---------------------------|-----------------------------------|-----------------------------------|---|---|---|---------------------|------------------------|---------|-----|
| | 0-1.5 | 1.5-2.5 | 2.5-4.5 | 4.5-6.0 | 6-7.5 | 7.5-9 | 9-10 | 10-12 | 12-30 | | |
| Material type | Silty Gravel/ Gravelly Sand | Silt/ Gravelly Silt | Silty Gravelly Sand/ Gravel | Gravel/ Gravelly silty Sand | Silt/ Sandy silt (liq) ¹ | Silty Gravel/ Gravelly silty sand | Silt/ Sandy silt (liq) ¹ | Silt/ Sandy Silt | Silt/ Sandy Silt | | |
| Material Model | HS D ² | HS D | HS D | HS D | HS D | HS UNB ³ | HS D | HS D | HS UNB ³ | HS D | |
| Unit weight γ (kN/m ³) | 20 | 19 | 20 | 20 | 18 | 20 | 18 | 20 | 20 | | |
| Initial void ratio e_{init} | 0.529 | 0.517 | 0.529 | 0.529 | 0.624 | 0.517 | 0.624 | 0.517 | 0.426 | | |
| E_{50}^{ref} (x 10 ³ MPa) | 122.3 | 45 | 55.87 | 50 | 15 | 2.55 | 38.39 | 15 | 2.7 | 45 | 170 |
| E_{oed}^{ref} (x 10 ³ MPa) | 122.3 | 55 | 55.87 | 50 | 9 | 1.53 | 38.39 | 9 | 1.62 | 55 | 230 |
| E_{ur}^{ref} (x 10 ³ MPa) | 366.8 | 135 | 167.6 | 150 | 45 | 7.65 | 115.2 | 45 | 8.1 | 135 | 510 |
| m | 0.5 | 0.75 | 0.5 | 0.5 | 1.0 | 0.5 | 1.0 | 0.75 | 0.5 | | |
| Cohesion c'_{ref} (kPa) | 2 | 20 | 2 | 5 | 12 | - | 5 | 2 | - | 20 | 100 |
| Friction angle ϕ' (°) | 30 | 35 | 33 | 30 | 33 | 0 | 30 | 33 | 0 | 35 | 34 |

| Parameters | Depth (m) | | | | | | | | | | |
|------------------------------------|-----------|---------|---------|---------|-------|-------|-------|--------|---------------|--------|-------|
| | 0-1.5 | 1.5-2.5 | 2.5-4.5 | 4.5-6.0 | 6-7.5 | 7.5-9 | 9-10 | 10-12 | 12-30 | | |
| Undrained strength kPa | - | - | - | - | - | 8 | - | - | 11 | - | |
| Dilatancy angle Ψ (°) | 4 | 6 | 4 | 4 | 0 | 4 | 0 | 6 | 6 – 1 w depth | | |
| Failure ratio R_f | 0.9 | 0.9 | 0.9 | 0.9 | 0.9 | 0.9 | 0.9 | 0.9 | 0.9 | | |
| Interface ratio R_{inter} | 0.7 | 0.7 | 0.7 | 0.7 | 0.7 | 0.7 | 0.7 | 0.7 | 0.7 | | |
| Poisson's ratio | 0.25 | 0.25 | 0.25 | 0.25 | 0.3 | 0.25 | 0.3 | 0.25 | 0.2 | | |
| Reference pressure P_{ref} (kPa) | 100 | 100 | 100 | 100 | 100 | 100 | 100 | 100 | 100 | | |
| At rest earth pressure K_0^{nc} | 0.529 | 0.426 | 0.455 | 0.529 | 0.45 | 1 | 0.517 | 0.56 | 1 | 0.426 | 0.441 |
| K_x (m/day) | 86.4 | 1.728 | 2.592 | 2.592 | 1.728 | 2.592 | 1.278 | 0.172 | 8 | 0.1728 | |
| K_y (m/day) | 86.4 | 0.864 | 1.296 | 1.296 | 0.864 | 1.296 | 0.864 | 0.0864 | 0.0864 | 0.0864 | |
| OCR | 1 | 1 | 1 | 1 | 1 | 1 | 1 | 1 | 1 | 1 | |

¹ Soil with liquefaction potential under ULS seismic loading, ² Hardening soil model – drained, ³ Hardening soil model – undrained
B – after liquefaction

3.2 Design loading

Design loading including dead (self-weight of the structure) and live loads (HN and HO loading as per NZTA Bridge Manual, crane loads provided by the Contractor), ground and groundwater loading were included in the Plaxis analysis. Cumulative cyclic seismic displacements were applied to the model boundaries in the seismic case.

3.3 Pile length calculations

The length of the piles was calculated to have the effective weight of soil mass at the toe elevation of the piles larger than the seepage forces (Knappett & Craig, 2019). This was accomplished by calculating the transient hydraulic gradient using GeoStudio Seep/W. This analysis resulted in 17m long piles. A reverse bearing capacity analysis to check the stability of the excavation during excavation was also completed.

3.4 Liquefaction uplift

MBIE Module 4 (MBIE, 2021) describes the effects of liquefaction at depth on a surficial raft or mat, with high fluid pressure being injected against the underside of the surface structure. These pressures may be very high particularly when the structure base is below grade and approximately equal to the total vertical stress at the depth of the liquefaction. The Plaxis 3D output provides the maximum of total vertical stress and mean total confining pressure, with the liquefaction uplift pressure under the concrete plug equated to that value. Tensile skin friction was assumed as 0.75 of the compressive skin friction (Reese, Isenhowe, & Wang, 2005), with no strength assumed for liquefied material, for both effective and total stress analysis. The total

weight of the shaft plus these stabilising forces were compared with the destabilising forces of the seismic uplift under the concrete plug plus the uplift forces under the piles.

In addition, bearing capacity at the base of the piles was checked assuming negative skin friction on the piles as a result of liquefaction of the overlying layers.

3.5 Plaxis Analysis

The primary analysis method for the pump station was a 3D FEM model using Plaxis 3D to model critical design stages including temporary and long term stability of the pump station, projected displacement of the existing adjacent structures, seismic analysis, sensitivity checks on soil stiffness and sensitivity to pile bearing loss of the adjacent carpark. The Plaxis model mesh is shown in Figure 2.

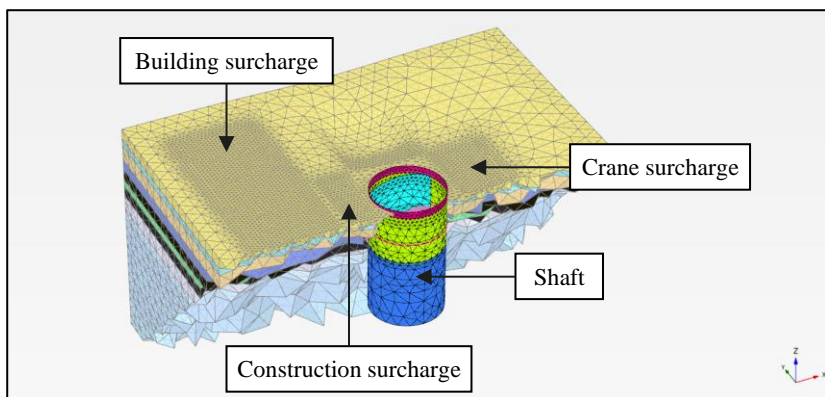


Figure 2: Plaxis model mesh

3.5.1 Model stages

Construction stages and sequencing was set up in the Plaxis model so that the correct stress path is followed and the locked in stresses are correctly modelled. Construction staging is summarised in Table 4.

Table 4: Plaxis 3D analysis stages

| Stage | Description |
|-------|--|
| 1 | Stress initialisation phase (K_0 stress condition). |
| 2 | Construction of the (existing) adjacent buildings. |
| 3 | Construction of the secant piles and application of the construction surcharges at the surface. |
| 4 | Dewatering and excavation of the shaft in 5 stages. |
| 5 | Construction of the base plug. |
| 6 | Construction of the internal walls and shotcrete lining. |
| 7 | Place lid. |
| 8 | Long term conditions (remove construction surcharges, HN loading applied, long term groundwater table applied, reduction of flexural stiffness of the secant piles by 50% to account for creep). |
| 9 | Application of seismic loading |
| 9.1 | Apply 1/100 year event at end of excavation, before plug placement |
| 9.2 | Apply 1/500 year event at end of excavation, before plug placement – to check adjacent building |

Stage Description

- 9.3 Apply 1/1,000 year event for long term conditions (SLS2)
9.4 Apply 1/2,500 year event for long term conditions (ULS)

In addition to the above analyses, a sensitivity check with 50% higher stiffness for the upper 7.5m of soil, and liquefaction beneath the piles of the existing adjacent carpark building and subsequent transfer of pile load to ground surface during an earthquake. This assumes that sudden loss of support is experienced by the carparking building piles and the suspended concrete floors exert the full load on the ground surface.

3.5.2 Model outputs

The Plaxis model outputs the axial forces, bending moments for the piles and the maximum horizontal hoop forces at each stage and were provided to the structural engineer to complete the structural design.

Figure 3 shows the Plaxis 3D displacement as a deformed mesh during a ULS (1/2,500 year) event, with a maximum total displacement of 1.079 m imposed on the boundaries. It also shows the total settlement of the surrounding area as the excavation of the shaft progressed including surcharges from the crane, general construction surcharges, and the adjacent building surcharges. Modelling the response of the surrounding structures in conjunction with construction stages enables more accurate settlement predictions and monitoring plans.

The results of the analysis also indicate that settlement of adjacent buildings due to construction and dewatering within the shaft is expected to be negligible. A robust settlement monitoring regime with trigger levels comprising settlement pins was implemented in conjunction with groundwater monitoring. Pre- and post- construction conditions surveys are also important to establish a baseline prior to construction to quantify existing damage.

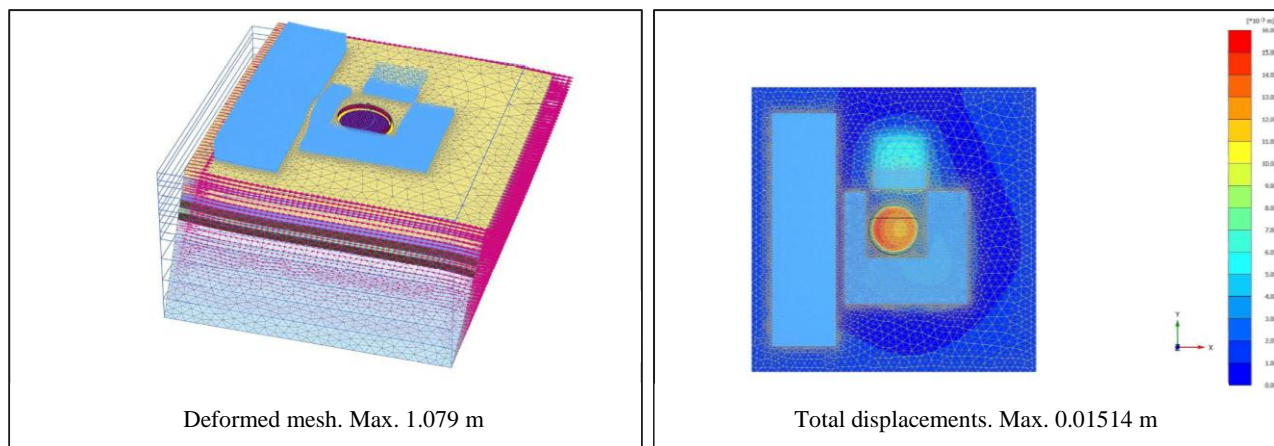


Figure 3: Example outputs of deformed mesh in ULS conditions and total settlement distribution during construction

Figure 4 and Figure 5 show the Plaxis outputs of the predicted static and seismic component of the lateral earth pressure distribution in the x-axis direction on the shaft piles.

Figure 4 shows the lateral stresses for the end of excavation, long term conditions, theoretical earth pressures for active and at rest (K_0) conditions. The graph shows the effective horizontal stress is larger than the theoretical at rest value but becomes closer to the theoretical value in the long term.

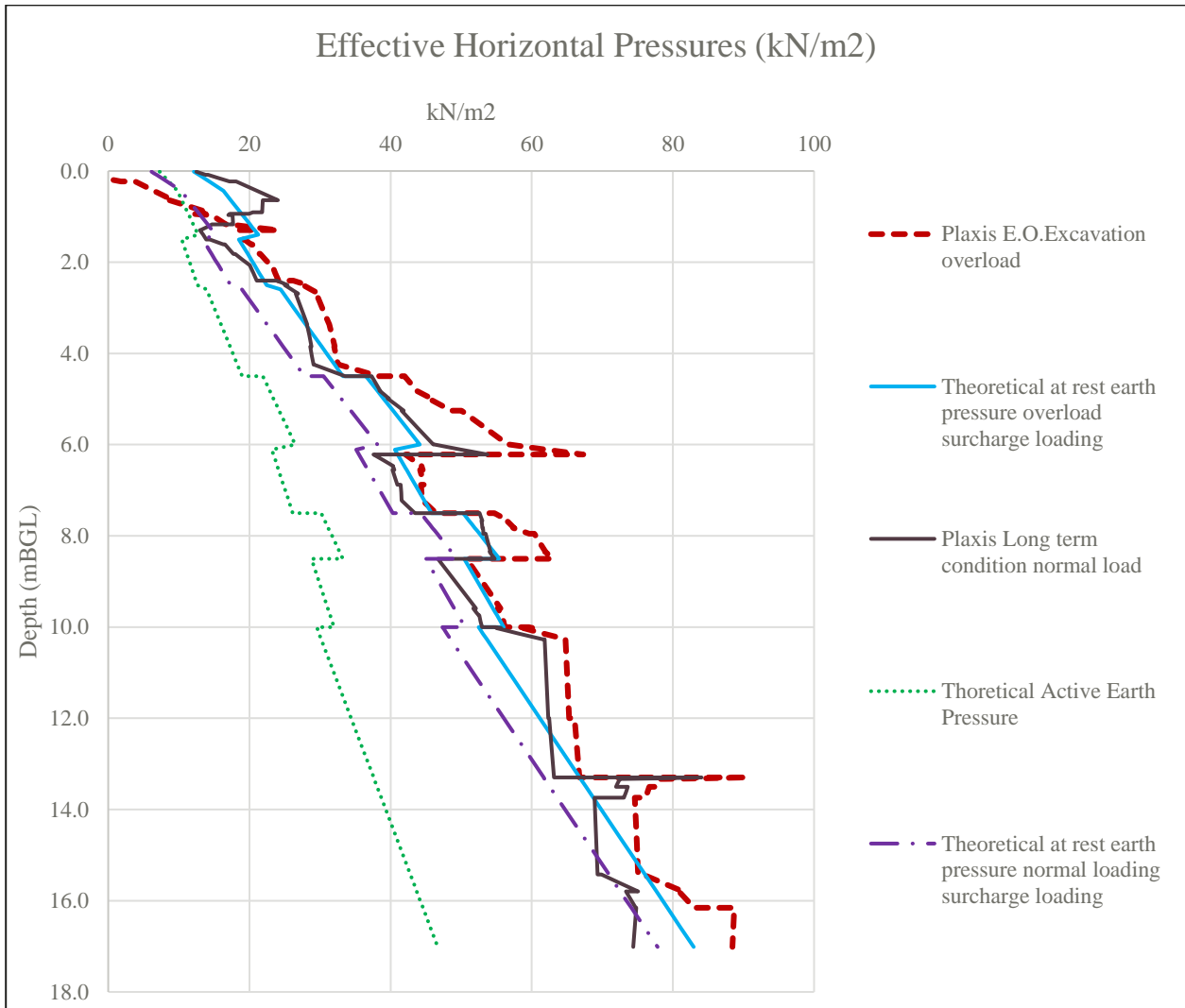


Figure 4: Effective horizontal pressures

Figure 5 shows the increase in the seismic earth pressure in the upper layers due to the liquefaction on the soil layer at 6 to 7.5m depth. The graph also shows that the structure is likely to perform as a flexible structure during seismic loading, as opposed to a stiff or rigid structure.

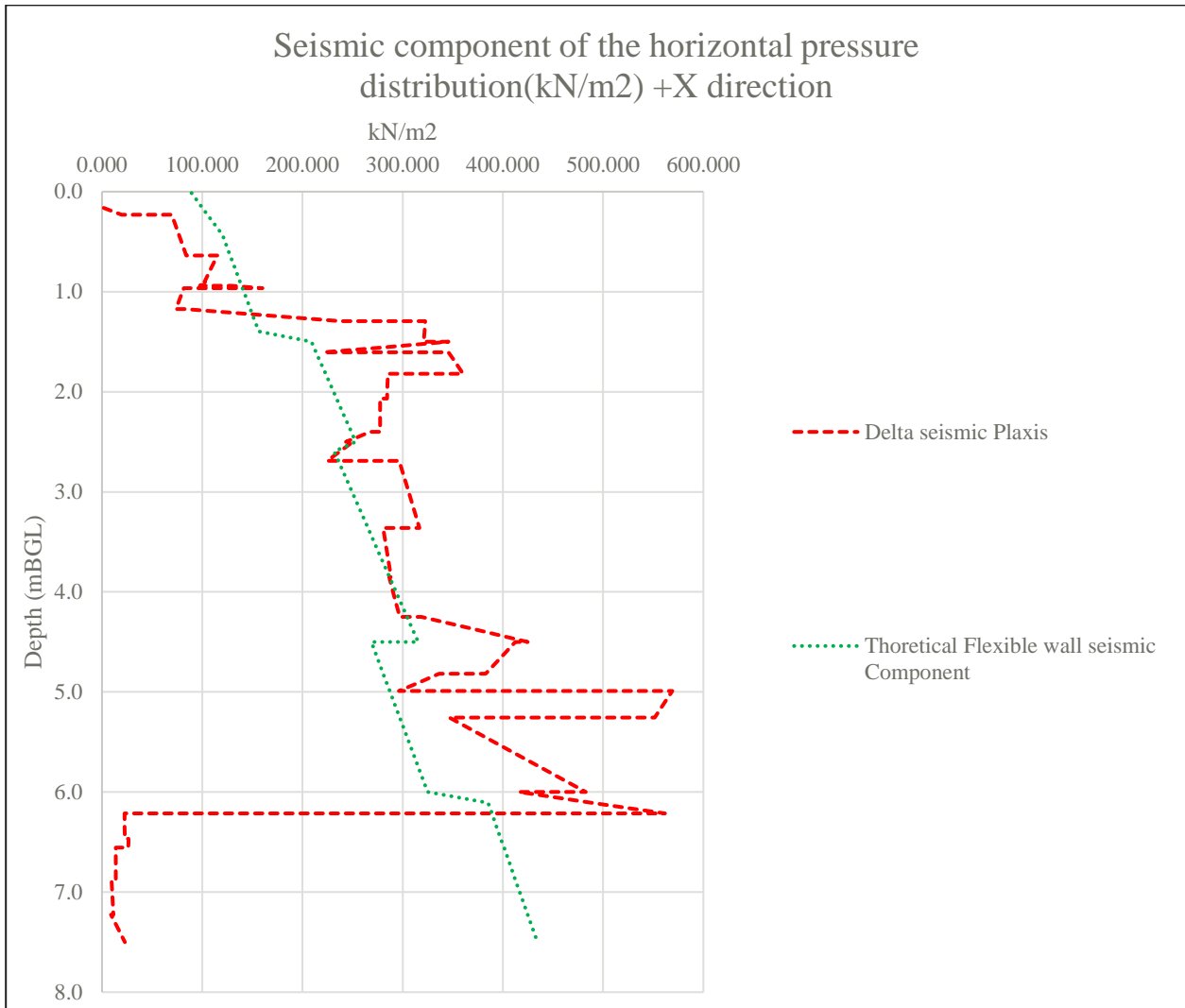


Figure 5: Seismic component of horizontal pressure distribution

4 CONCLUSION

Design of a large underground structure in challenging ground conditions requires multiple inputs and consideration of concurrently acting forces in a staged approach. To adequately complete these analyses using conventional methods is time consuming and has a high degree of difficulty. Finite element modelling using Plaxis 3D allows thorough analysis of the proposed structure and outputs of loads on the shaft for structural design, systematic assessment of excavation and structure stability during each construction stage, and quantifies the effects on adjacent sensitive structures with a high degree of confidence.

5 ACKNOWLEDGEMENTS

The authors would like to acknowledge GHD Limited and Wellington Water Limited for their support and permission to publish on the Taranaki Street Pump Station project. The detailed design work was completed during the authors' time at GHD.

6 REFERENCES

- Balachandra, A. (2021). *Taranaki Street Pump Station Seismic Hazard Assessment*. Tonkin and Taylor.
- Begg, J. G., & Mazengarb, C. (1996). *Geology of the Wellington Area, scale 1:50,000. Institute of Geological & Nuclear Sciences geological map 10. 1 sheet + 64 p.* Lower Hutt: Institute of Geological & Nuclear Sciences Limited.
- Boulanger, R. W., & Idriss, I. M. (2014). *CPT and SPT based liquefaction triggering procedures*. University of California at Davis, Department of Civil & Environmental Engineering, Davis.
- Clayton, C. R. (1995). *The standard penetration test (SPT): methods and use (R143)*. CIRIA.
- Knappett, J., & Craig, R. F. (2019). *Craig's Soil Mechanics* (9th ed.). CRC Press.
- MBIE. (2021, November). Earthquake geotechnical engineering practice, Module 1. *Overview of the guidelines*.
- MBIE. (2021, November). Earthquake geotechnical engineering practice, Module 4. *Earthquake resistant foundation design*.
- NZS. (2002). NZS1170.0:2002 Part 0: General Actions.
- NZS. (2004). NZS1170.5:2004 Part 5: Earthquake actions.
- Reese, L. C., Isenhower, W. M., & Wang, S.-T. (2005). *Analysis and Design of Shallow and Deep Foundations*. Hoboken, New Jersey, USA: John Wiley & Sons, Inc. doi:10.1002/9780470172773
- Stark, T. D., & Mesri, G. (1992). Undrained Shear Strength of Liquefied Sands for Stability Analysis. *Journal of Geotechnical Engineering*, 118, 1727-1747. doi:10.1061/(ASCE)0733-9410(1992)118:11(1727)